Using EMD-FrFT Filtering to Mitigate Very High Power Interference in Chirp Tracking Radars

Sherif A. Elgamel, *Student Member, IEEE*, and John J. Soraghan, *Senior Member, IEEE*

***Abstract*—This letter presents a new signal processing subsystem for conventional monopulse tracking radars that offers an improved solution to the problem of dealing with manmade high power interference (jamming). It is based on the hybrid use of empirical mode decomposition (EMD) and fractional Fourier transform (FrFT). EMD-FrFT filtering is carried out for complex noisy radar chirp signals to decrease the signal's noisy components. An improvement in the signal-to-noise ratio (SNR) of up to 18 dB for different target SNRs is achieved using the proposed EMD-FrFT algorithm.**

***Index Terms*—Empirical mode decomposition, fractional Fourier transforms, high power interference suppression.**

I. Introduction

A high power noise interference introduced to a monopulse tracking radar processor through the radar antenna produces an interference error that affects the radar tracking ability and may cause target mistracking [1]. Various methods [2]–[4] for combating high noise power interference have been published.

In our previous work [1] the mistracking problem due to interference signals was addressed using the filtering in the Fractional Fourier Transform domain. In this letter we propose the use of both empirical mode decomposition (EMD) and fractional Fourier transform (FrFT) to implement N EMD-FrFT filters in an attempt to reduce the very high power interference signals introduced from the antenna main lobe or from the antenna side lobes for N radar receiving channels. Following a brief introduction on EMD and FrFT the letter then describes the structure of the new EMD-FrFT filtering algorithm based monopulse radar processor. The superior performance of the new algorithm is demonstrated using a set of simulation results.

II. Classical and Bivariate EMD

The intrinsic mode functions (IMFs) of an EMD signal decomposition are oscillatory and have no DC component, so the signal $\boldsymbol{x}[n]$ in the EMD domain may be represented as [5]

$$\boldsymbol{x}[n] = \sum_{i=1}^{L} \boldsymbol{h}^{(i)}[n] + \boldsymbol{d}[n] \tag{1}$$

where $\boldsymbol{h}^{(i)}[n]$, are the L IMFs $1 \leq i \leq L$ and $\boldsymbol{d}[n]$ is the residual. When a signal $\boldsymbol{x}[n]$, comprising a slow oscillation superimposed on a highly oscillating signal (in our case additive high power interference noise signal), is applied to an EMD algorithm, the first few IMFs tend to contain the highly oscillation signal (noise) and the remaining IMFs contain the useful signal (in our case radar chirp signal).

The bivariate EMD [6] may be used for complex valued time series. As with the classical EMD, the bivariate EMD is used to separate the more rapidly rotating components from slower ones. The procedure is to define the slowly rotating component as the mean of some envelope which is a three-dimensional cylinder that encloses the signal. In our work the bivariate EMD (complex EMD) is used to decompose the complex radar signal into a complete and finite set of complex IMFs in order to subsequently minimise the additive noise interference.

The concept of detrending in high frequency noise environments is to calculate an estimate of the IMF number at which all previous IMFs may be regarded as noise and the subsequent IMFs may be considered to contain the useful signal components.

The IMF detrending technique assumes that the 1st IMF, $\boldsymbol{h}^{(1)}[n]$, captures mostly noise, the noise level $\hat{W}[1]$ is estimated in $x[n]$ by computing [5]

$$\hat{W}[1] = \sum_{n=1}^{N_s} \left(\boldsymbol{h}^{(1)}[n]\right)^2 \tag{2}$$

where N_s is the number of samples. The model for noise only IMF energies can be approximated for white Gaussian noise dependence on the energy of the first IMF $h^{(1)}[n]$ from [5]

$$\hat{W}[i] = \frac{\hat{W}[1]}{0.719} \times 2.01^i \qquad 2 \leq i \leq L. \tag{3}$$

The threshold level energies $T[i]$ are used to distinguish between signal and noise. They are calculated using the approximated IMF energies in (3) from [5]

$$\log_2\left(\log_2\left(\frac{T[i]}{\hat{W}[i]}\right)\right) = 0.46i - 1.92 \quad 2 \leq i \leq L. \tag{4}$$

Computing the IMFs energies by applying the EMD algorithm on $\boldsymbol{x}[n]$ (noisy signal) from [5]

$$W[i] = \sum_{n=1}^{N_s} \left(\boldsymbol{h}^{(i)}[n]\right)^2 \qquad 2 \leq i \leq L. \tag{5}$$

Comparing IMFs energies $W[i]$ with the threshold level energies $T[i]$ allows us to determine exactly when the signal energy level crosses the threshold level.

Assuming this occurs at $i = m$, the signal $\boldsymbol{x}[n]$ is denoised by reconstruction using only IMFs whose energy exceeds the threshold according to:

Manuscript received November 30, 2010; revised January 27, 2011; accepted February 07, 2011. The associate editor coordinating the review of this manuscript and approving it for publication was Prof. Amir Asif.

The authors are with The Centre for Excellence in Signal and Image Processing, Department of Electronic and Electrical Engineering, University of Strathclyde, Glasgow, U.K. (e-mail: sherifelgamel73@gmail.com; j.soraghan@eee.strath.ac.uk).

Color versions of one or more of the figures in this paper are available online at http://ieeexplore.ieee.org.

Digital Object Identifier 10.1109/LSP.2011.2115239

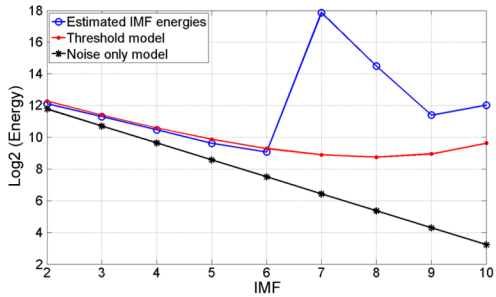

Fig. 1. Detrending and the thresholding.

$$\widetilde{\boldsymbol{x}}[n] = \sum_{i=m+1}^{L} \boldsymbol{h}^{(i)}[n] + \boldsymbol{d}[n]. \tag{6}$$

In Fig. 1 the EMD algorithm is applied to a noisy signal resulting in 10 IMFs. Using (2) and (3) the 1st IMF is used to estimate the noise only energies for the remaining IMFs. The resulting noise only model outputs are shown in Fig. 1. The actual IMFs energies calculated from (5) are also illustrated on Fig. 1 along with the threshold model for each IMF. It is clear that the actual IMFs energies are close to those estimated for the noise only model up to IMF 6 at which the threshold level is crossed. This means that these IMFs (from 1 to 6) may be regarded as essentially noise only. Thus, the sum of IMFs from 7 to 10 represents the detrended and thresholded signal.

For the noisy signal, a higher sampling frequency yields a higher number of samples and as a result a greater number of IMFs using the EMD algorithm. Consequently a higher accuracy of detrending IMFs in the EMD-DT algorithm is expected. This concept of detrending and thresholding is used later in Section V.

III. Fractional Fourier Transform

The fractional Fourier transform of order a of an arbitrary function $x(t)$, with an angle α is defined as [7], [8]

$$X_\alpha(t_a) = \int_{-\infty}^{\infty} x(t) K_\alpha(t, t_a) dt \tag{7}$$

where $K_\alpha(t, t_a)$ is the transformation kernel, t_a is the transformation of t to the a^{th} order, and $\alpha = a\pi/2$ with $a \in \Re$. The optimum order value,a_{opt} for a chirp signal may be computed as [9]

$$a_{opt} = -\frac{2}{\pi} \tan^{-1}\left(\frac{F_s^2 T}{\Delta f L_s}\right) \tag{8}$$

where F_s is the sampling frequency, T is the chirp duration, L_s is the number of samples in the time received window, and Δf is the chirp bandwidth.

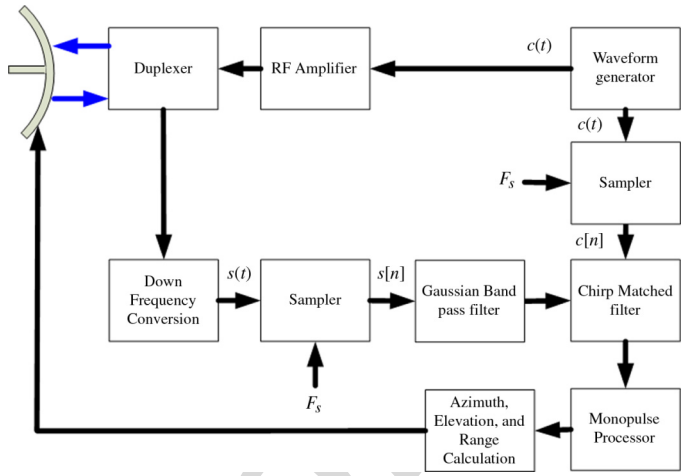

Fig. 2. Basic structure of monopulse radar.

IV. Monopulse Radar Signal

A block diagram of a typical monopulse radar is shown in Fig. 2. A pulsed chirp signal $c(t)$ is produced from the waveform generator. This is up-converted to the radar carrier frequency, amplified and passed through the duplexer to be transmitted:

$$c(t) = \exp\left(j\pi\left(\frac{F_{stop} - F_{start}}{T}\right)\left(t - \frac{T}{2}\right)^2\right) \tag{9}$$

where t is the time, F_{start} is the chirp start frequency, and F_{stop} is the chirp stop frequency. This is up-converted to the radar carrier frequency, amplified and passed through the duplexer to be transmitted. The down-converted received signal passes through a band limited Gaussian before passing through the chirp matched filter to maximize the target return signal. The target information parameters (azimuth angle, elevation angle, and target range) are then calculated by the monopulse processor from the filtered signal.

The structure of monopulse radar shown in Fig. 2 is repeated N times (N equal to the of array antenna elements). Thus each antenna will have its own complete receiving system and all the output data will be processed using only one monopulse processor.

The radar received chirp signal $s(t)$ may be expressed in the baseband as [1] shown in the equation at bottom of page, where A is the received signal amplitude, ϕ_o is a random phase shift, $\boldsymbol{F}_d$ is the Doppler vector, $\boldsymbol{F}_\phi$ is antenna phase factor, and T_{start} is the start time of the returned pulse.

The start time T_{start} depends on the target range R_t and can be computed from

$$T_{start} = \frac{2 \times R_t}{c} \tag{11}$$

where c is the speed of light. As indicated in (10) the Doppler shift and delay effect on the target chirp signal is determined

$$s(t) = \begin{cases} \left[\left(Ae^{-j2\pi\phi_o} e^{j\pi\left(\frac{F_{stop}-F_{start}}{T}\right)\left(t-T_{start}-\frac{T}{2}\right)^2}\right).\boldsymbol{F}_d\right] \times \boldsymbol{F}_\phi, & T_{start} < t < T_{start} + T \\ 0, & elsewhere \end{cases} \tag{10}$$

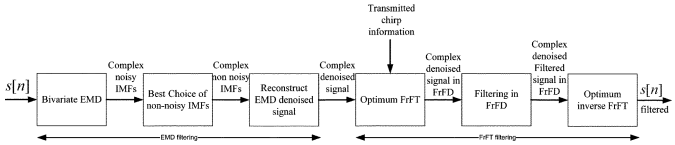

Fig. 3. EMD-FrFT filtering.

by the dot product of the chirp signal by the Doppler vector $\boldsymbol{F}_d$ defined as

$$\boldsymbol{F}_d = \exp\left(j2\pi f_d(t - T_{start})\right) \tag{12}$$

where f_d is the target Doppler frequency.

For the phased array receiving antenna, an antenna phase factor $\boldsymbol{F}_\phi$ is introduced as

$$\boldsymbol{F}_\phi = \exp\left(-j2\pi f_c(T_{start}\boldsymbol{I} - \boldsymbol{N_{array}}\Delta t)\right) \tag{13}$$

where $\boldsymbol{N_{array}}$ is a vector represented as $\{0, 1, \ldots\ldots, N-1\}$, $\boldsymbol{I}$ is a $1 \times N$ unitary vector, and Δt is calculated from

$$\Delta t = D \sin \phi_t / c \tag{14}$$

where D is the separation between the antenna elements, ϕ_t is the target angle from the antenna boresight.

V. Filtering Based EMD-FrFT Algorithm

It is proposed to combat the high power noise interference by filtering the received signal in the optimal fractional Fourier transform (FrFT) domain using the transmitted chirp radar information. Normally the magnitude of chirp signal in the optimum FrFT domain would be significantly higher than the noise signal in the fractional domain [1]. However in high power jamming scenarios this is not usually true and it becomes difficult to distinguish between the target spike and the noise spikes in the optimal FrFT domain.

The proposed EMD-FrFT radar filtering process, which must be applied to the received signal before the band pass filter, is shown in Fig. 3. The radar received noisy complex chirp signal $s(t)$ is sampled using the radar sampling frequency to form $s[n]$. The $s[n]$ signal recovery is carried out in two stages: i) EMD Filtering Stage and ii) the FrFT Filtering Stage.

EMD Filtering Stage: In stage one the received signal $s[n]$ is input to a bivariate EMD to produce the complex IMFs $\boldsymbol{h}^{(i)}[n]$. The complex IMFs are detrended and thresholded to estimate the non-noisy IMFs using (2)–(5) as described in Section II. Only IMFs whose energy exceeds the threshold are retained. The resultant thresholded IMFs are combined to produce the complex denoised signal as in (6).

FrFT Filtering Stage [1]: For the second stage, the complex denoised signal in the optimal fractional domain is calculated from the information supplied from the transmitted chirp signal as in (8). Knowing the peak position of the target chirp signal in the optimum FrFT domain, the received data is filtered by keeping the chirp target data (peak position sample and its adjacent samples) and forces all the remaining samples in the tracking window to zero. The inverse FrFT is used with the known optimal order to transform the signal back to time domain after filtering. The EMD-FrFT filtered data is supplied to the radar processor to continue data processing to calculate the target information.

The EMD-FrFT filtering process illustrated in Fig. 3 is attached to N receiving channels in which the received signal from each of the N antenna elements will fill L_s range gates.

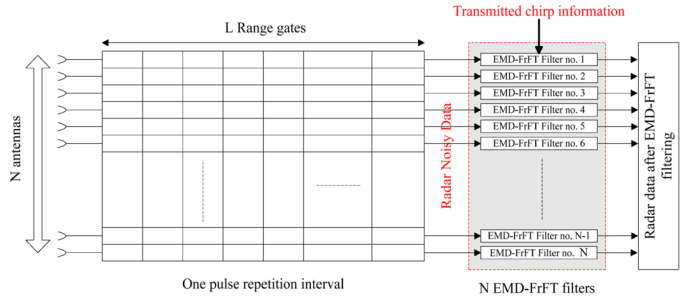

Fig. 4. Radar data EMD-FrFT filtering.

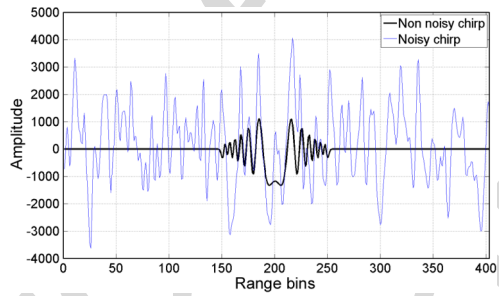

Fig. 5. High noisy chirp signal in time domain (real).

The total radar data size is therefore equal to $N \times L_s$ for each pulse return. The EMD-FrFT filter block seen in Fig. 4 consists of N EMD-FrFT filters shown in Fig. 3. The overall filtered data $(N \times L_s)$ are processed to determine the target information parameters as illustrated in Fig. 2.

VI. Simulation Results

The computer based simulations comprise an array of 14 elements spaced 1/3 m apart. The radar pulse width is 100 microseconds and a pulse repetition interval of 1.6 ms for a 435 MHz carrier was used. The incoming baseband signals are sampled at 1 MHz. Also it is assumed that the radar operating range is 100:200 range bins with a starting window at 865 μm and a window duration of 403 μm. The target is considered at range bin $=$ 150 at angle 32° from the look direction with target signal to noise ratio (SNR) set to 56 dB. A jamming signal with interference noise ratio (INR) set to 75 dB at angle 32° from the look direction (main beam jamming) is introduced.[1]

A. High Power Interference Scenario

Considering the simulation parameters for one of the 14 receiving channels (first channel), the receiving target chirp signal appears at range bin 150 in case of no jamming while the chirp signal is completely corrupted in the time domain (also in the frequency domain) by the noise due to high power jamming signal as seen in Fig. 5.

The bivariate EMD is applied to the noisy signal to produce the complex IMFs. A sampling frequency is increased to 10 MHz (ten times the radar sampling frequency F_s) to increase the number of IMFs.

The resultant complex IMFs from applying the bivariate EMD to the noisy chirp 1×4029 produces 14 IMFs each of length 4029. Keeping only IMFs whose energy exceeds the threshold using the EMD-DT algorithm described in Section II the signal is reconstructed summing the non-noisy IMFs from

[1]The simulations parameters are extracted from DARPA/Navy Mountaintop Program. See URL http://spib.rice.edu/spib/mtn_top.html.

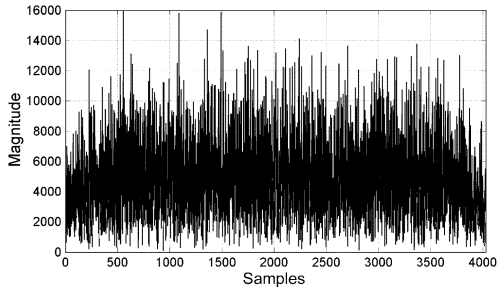

Fig. 6. High noisy chirp signal in optimum FrFD.

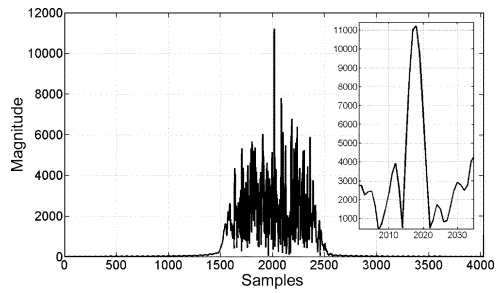

Fig. 7. EMD denoised chirp in optimum FrFD.

6 to 14 to obtain the filtered signal after applying EMD-DT algorithm.

Substituting the monopulse radar parameter values given above into (8) with a high sampling frequency of 10 MHz, the order of the optimal FrFT domain a_{opt} is computed as 1.1266. The EMD filtered signal is transferred to the optimal FrFD using the optimal order FrFT domain a_{opt} 1.1266.

Transforming the radar received signal directly to the optimum FrFD using the calculated a_{opt}, is expected to produce a high magnitude value (spike) due to transferring the chirp signal to the optimum FrFD. However as seen in Fig. 6 due to the high power interference the spike of the target chirp is highly corrupted also by noise spikes in the optimum FrFD and cannot be filtered in this domain.

It is therefore difficult to distinguish between the target spike and the noise spikes in the optimal FrFD. The proposed EMD-FrFT filtering algorithm is used to address this problem. Fig. 7 shows the EMD denoised chirp in optimum FrFD. It is evident that the noise is significantly reduced especially the high frequency components and the chirp target spike is also the highest spike which is shown in the zoomed portion of Fig. 7.

The proposed filtering algorithm in the optimum FrFD keeps the sample with maximum magnitude (sample no. 2018) and its ten adjacent samples from 2013–2023 while forcing all other samples window to zero. The filtered signal is then transformed back to time domain by applying inverse optimum FrFT using—a_{opt} (-1.1266) by applying (7). The real and imaginary parts of the denoised signal (recovered) after applying the proposed EMD-FrFT filtering algorithm is shown in Fig. 3.

Fig. 8 compares the denoised chirp signal using EMD-FrFT filter with the non noisy signal. In the simulation example, the considered signal total input SNR is approximately equal -8 dB (after adding the jamming noise) and the output SNR is approximately 10 dB. The proposed EMD-FrFT filtering algorithm offers signal enhancement of approximately 18 dB.

B. Signal Improvement at Different SNR

Table I shows the improvement results of applying different target SNR for the same jamming scenario (INR set to 75 dB

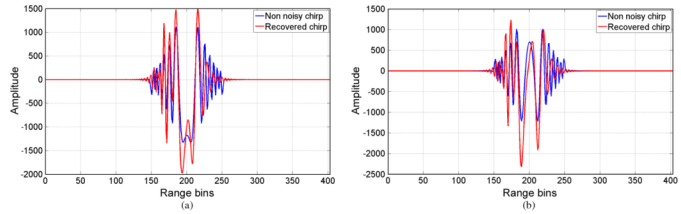

Fig. 8. Recovered chirp signal. (a) Real; (b) imaginary.

TABLE I
THE IMPROVEMENT RESULTS IN dB FOR MONOPULSE PROCESSORS

Input SNR	-7.7	-5.6	-2.9	-1.8	0.2	1.7	5.6	10.6
Output SNR	10.4	10.8	13	13.4	14.8	15.4	15.8	15.5
Gain	18.1	16.4	15.9	15.2	14.6	13.7	10.2	4.9

at angle 32°) and calculating the total input SNRs to the radar receiving channel. The results in Table I comprise an average over 50 independent noise generations.

Table I indicates an improvement of approximately 18.1 dBs for input SNR $= -7.7$ dB and an improvement of approximately 4.9 dBs for input SNR $= 10.6$ dB. The proposed EMD-FrFT algorithm yields a higher improvement for the lower SNRs rather than the higher SNRs.

VII. CONCLUSION

A system to reduce the distortion problem due to high power interference in chirp radar systems is presented. The proposed EMD-FrFT filtering algorithm successfully decreases the high power noise interference and improves the received radar SNR. A resulting improvement in the radar received signal is obtained for different SNR and the highest gain is achieved in the case of lower SNR (up to 18 dB in the considered case).

REFERENCES

[1] S. A. Elgamel and J. J. Soraghan, "Enhanced monopulse radar tracking using fractional fourier filtering in the presence of interference," in *11th Int. Radar Symp. (IRS), 2010 11th International*, 2010, pp. 1–4.

[2] A. Farina, G. Golino, and L. Timmoneri, "Maximum likelihood estimator approach to determine the target angular co-ordinates in presence of main beam interference: Application to live data acquired with a microwave phased array radar," in *IEEE Int. Radar Conf.*, 2005, pp. 61–66.

[3] Y. Seliktar, E. J. Holder, and D. B. Williams, *A Space/Fast-Time Adaptive Monopulse Technique*. New York: Hindawi, 2006, pp. 218–228.

[4] J. Zongsheng and S. Xicai, "Analysis on the tracking performance of active radar seeker under the condition of coherent interference," in *IEEE Int. Conf. Intelligent Computing and Intelligent Systems*, 2009, pp. 418–422.

[5] P. Flandrin, P. Goncalves, and G. Rilling, "Detrending and denoising with empirical mode decompositions," in *2004 Eur. Signal Processing Conf. (EUSIPCO-2004)*, 2004.

[6] G. Rilling, P. Flandrin, P. Gonalves, and J. M. Lilly, "Bivariate empirical mode decomposition," *IEEE Signal Process. Lett.*, vol. 14, pp. 936–939, 2007.

[7] C. Candan, M. A. Kutay, and H. M. Ozaktas, "The discrete fractional fourier transform," *IEEE Trans. Signal Process.*, vol. 48, pp. 1329–1337, 2000.

[8] H. M. Ozaktas, G. Zalevsky, and M. A. Kutay, *The Fractional Fourier Transform: With Applications in Optics and Signal Processing*. New York: Wiley, Jan. 2001.

[9] C. Capus and K. Brown, "Short-time fractional fourier methods for the time-frequency representation of chirp signals," *J. Acoust. Soc. Amer.*, vol. 113, no. 6, pp. 3253–3263, 2003.

Using EMD-FrFT Filtering to Mitigate Very High Power Interference in Chirp Tracking Radars

Sherif A. Elgamel, *Student Member, IEEE*, and John J. Soraghan, *Senior Member, IEEE*

***Abstract*—This letter presents a new signal processing subsystem for conventional monopulse tracking radars that offers an improved solution to the problem of dealing with manmade high power interference (jamming). It is based on the hybrid use of empirical mode decomposition (EMD) and fractional Fourier transform (FrFT). EMD-FrFT filtering is carried out for complex noisy radar chirp signals to decrease the signal's noisy components. An improvement in the signal-to-noise ratio (SNR) of up to 18 dB for different target SNRs is achieved using the proposed EMD-FrFT algorithm.**

***Index Terms*—Empirical mode decomposition, fractional Fourier transforms, high power interference suppression.**

I. Introduction

A high power noise interference introduced to a monopulse tracking radar processor through the radar antenna produces an interference error that affects the radar tracking ability and may cause target mistracking [1]. Various methods [2]–[4] for combating high noise power interference have been published.

In our previous work [1] the mistracking problem due to interference signals was addressed using the filtering in the Fractional Fourier Transform domain. In this letter we propose the use of both empirical mode decomposition (EMD) and fractional Fourier transform (FrFT) to implement N EMD-FrFT filters in an attempt to reduce the very high power interference signals introduced from the antenna main lobe or from the antenna side lobes for N radar receiving channels. Following a brief introduction on EMD and FrFT the letter then describes the structure of the new EMD-FrFT filtering algorithm based monopulse radar processor. The superior performance of the new algorithm is demonstrated using a set of simulation results.

II. Classical and Bivariate EMD

The intrinsic mode functions (IMFs) of an EMD signal decomposition are oscillatory and have no DC component, so the signal $\boldsymbol{x}[n]$ in the EMD domain may be represented as [5]

$$\boldsymbol{x}[n] = \sum_{i=1}^{L} \boldsymbol{h}^{(i)}[n] + \boldsymbol{d}[n] \tag{1}$$

where $\boldsymbol{h}^{(i)}[n]$, are the L IMFs $1 \leq i \leq L$ and $\boldsymbol{d}[n]$ is the residual. When a signal $\boldsymbol{x}[n]$, comprising a slow oscillation superimposed on a highly oscillating signal (in our case additive high power interference noise signal), is applied to an EMD algorithm, the first few IMFs tend to contain the highly oscillation signal (noise) and the remaining IMFs contain the useful signal (in our case radar chirp signal).

The bivariate EMD [6] may be used for complex valued time series. As with the classical EMD, the bivariate EMD is used to separate the more rapidly rotating components from slower ones. The procedure is to define the slowly rotating component as the mean of some envelope which is a three-dimensional cylinder that encloses the signal. In our work the bivariate EMD (complex EMD) is used to decompose the complex radar signal into a complete and finite set of complex IMFs in order to subsequently minimise the additive noise interference.

The concept of detrending in high frequency noise environments is to calculate an estimate of the IMF number at which all previous IMFs may be regarded as noise and the subsequent IMFs may be considered to contain the useful signal components.

The IMF detrending technique assumes that the 1st IMF, $\boldsymbol{h}^{(1)}[n]$, captures mostly noise, the noise level $\hat{W}[1]$ is estimated in $x[n]$ by computing [5]

$$\hat{W}[1] = \sum_{n=1}^{N_s} \left(\boldsymbol{h}^{(1)}[n]\right)^2 \tag{2}$$

where N_s is the number of samples. The model for noise only IMF energies can be approximated for white Gaussian noise dependence on the energy of the first IMF $h^{(1)}[n]$ from [5]

$$\hat{W}[i] = \frac{\hat{W}[1]}{0.719} \times 2.01^i \qquad 2 \leq i \leq L. \tag{3}$$

The threshold level energies $T[i]$ are used to distinguish between signal and noise. They are calculated using the approximated IMF energies in (3) from [5]

$$\log_2\left(\log_2\left(\frac{T[i]}{\hat{W}[i]}\right)\right) = 0.46i - 1.92 \quad 2 \leq i \leq L. \tag{4}$$

Computing the IMFs energies by applying the EMD algorithm on $\boldsymbol{x}[n]$ (noisy signal) from [5]

$$W[i] = \sum_{n=1}^{N_s} \left(\boldsymbol{h}^{(i)}[n]\right)^2 \qquad 2 \leq i \leq L. \tag{5}$$

Comparing IMFs energies $W[i]$ with the threshold level energies $T[i]$ allows us to determine exactly when the signal energy level crosses the threshold level.

Assuming this occurs at $i = m$, the signal $\boldsymbol{x}[n]$ is denoised by reconstruction using only IMFs whose energy exceeds the threshold according to:

Manuscript received November 30, 2010; revised January 27, 2011; accepted February 07, 2011. The associate editor coordinating the review of this manuscript and approving it for publication was Prof. Amir Asif.

The authors are with The Centre for Excellence in Signal and Image Processing, Department of Electronic and Electrical Engineering, University of Strathclyde, Glasgow, U.K. (e-mail: sherifelgamel73@gmail.com; j.soraghan@eee.strath.ac.uk).

Color versions of one or more of the figures in this paper are available online at http://ieeexplore.ieee.org.

Digital Object Identifier 10.1109/LSP.2011.2115239

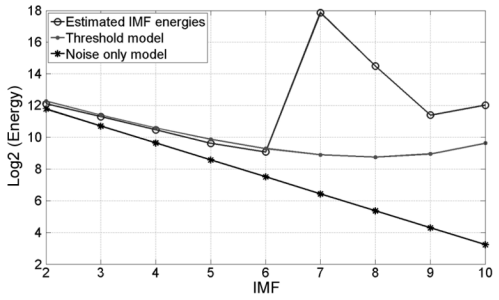

Fig. 1. Detrending and the thresholding.

$$\widetilde{\boldsymbol{x}}[n] = \sum_{i=m+1}^{L} \boldsymbol{h}^{(i)}[n] + \boldsymbol{d}[n]. \tag{6}$$

In Fig. 1 the EMD algorithm is applied to a noisy signal resulting in 10 IMFs. Using (2) and (3) the 1st IMF is used to estimate the noise only energies for the remaining IMFs. The resulting noise only model outputs are shown in Fig. 1. The actual IMFs energies calculated from (5) are also illustrated on Fig. 1 along with the threshold model for each IMF. It is clear that the actual IMFs energies are close to those estimated for the noise only model up to IMF 6 at which the threshold level is crossed. This means that these IMFs (from 1 to 6) may be regarded as essentially noise only. Thus, the sum of IMFs from 7 to 10 represents the detrended and thresholded signal.

For the noisy signal, a higher sampling frequency yields a higher number of samples and as a result a greater number of IMFs using the EMD algorithm. Consequently a higher accuracy of detrending IMFs in the EMD-DT algorithm is expected. This concept of detrending and thresholding is used later in Section V.

III. Fractional Fourier Transform

The fractional Fourier transform of order a of an arbitrary function $x(t)$, with an angle α is defined as [7], [8]

$$X_\alpha(t_a) = \int_{-\infty}^{\infty} x(t) K_\alpha(t, t_a) dt \tag{7}$$

where $K_\alpha(t, t_a)$ is the transformation kernel, t_a is the transformation of t to the a^{th} order, and $\alpha = a\pi/2$ with $a \in \Re$. The optimum order value,a_{opt} for a chirp signal may be computed as [9]

$$a_{opt} = -\frac{2}{\pi} \tan^{-1}\left(\frac{F_s^2 T}{\Delta f L_s}\right) \tag{8}$$

where F_s is the sampling frequency, T is the chirp duration, L_s is the number of samples in the time received window, and Δf is the chirp bandwidth.

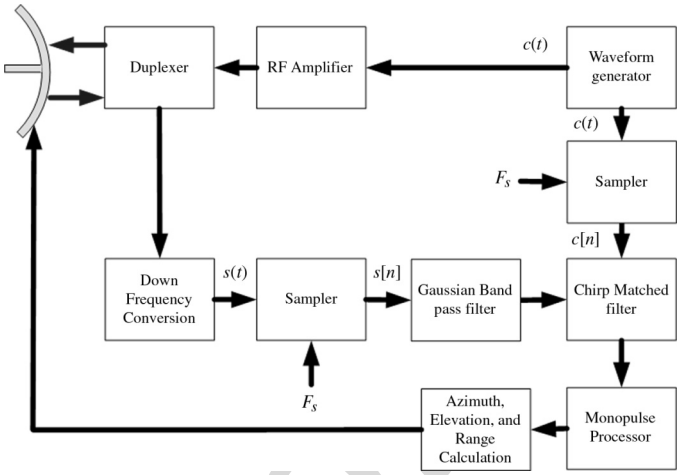

Fig. 2. Basic structure of monopulse radar.

IV. Monopulse Radar Signal

A block diagram of a typical monopulse radar is shown in Fig. 2. A pulsed chirp signal $c(t)$ is produced from the waveform generator. This is up-converted to the radar carrier frequency, amplified and passed through the duplexer to be transmitted:

$$c(t) = \exp\left(j\pi\left(\frac{F_{stop} - F_{start}}{T}\right)\left(t - \frac{T}{2}\right)^2\right) \tag{9}$$

where t is the time, F_{start} is the chirp start frequency, and F_{stop} is the chirp stop frequency. This is up-converted to the radar carrier frequency, amplified and passed through the duplexer to be transmitted. The down-converted received signal passes through a band limited Gaussian before passing through the chirp matched filter to maximize the target return signal. The target information parameters (azimuth angle, elevation angle, and target range) are then calculated by the monopulse processor from the filtered signal.

The structure of monopulse radar shown in Fig. 2 is repeated N times (N equal to the of array antenna elements). Thus each antenna will have its own complete receiving system and all the output data will be processed using only one monopulse processor.

The radar received chirp signal $s(t)$ may be expressed in the baseband as [1] shown in the equation at bottom of page, where A is the received signal amplitude, ϕ_o is a random phase shift, $\boldsymbol{F}_d$ is the Doppler vector, $\boldsymbol{F}_\phi$ is antenna phase factor, and T_{start} is the start time of the returned pulse.

The start time T_{start} depends on the target range R_t and can be computed from

$$T_{start} = \frac{2 \times R_t}{c} \tag{11}$$

where c is the speed of light. As indicated in (10) the Doppler shift and delay effect on the target chirp signal is determined

$$s(t) = \begin{cases} \left[\left(Ae^{-j2\pi\phi_o} e^{j\pi\left(\frac{F_{stop}-F_{start}}{T}\right)\left(t-T_{start}-\frac{T}{2}\right)^2}\right).\boldsymbol{F}_d\right] \times \boldsymbol{F}_\phi, & T_{start} < t < T_{start} + T \\ 0, & elsewhere \end{cases} \tag{10}$$

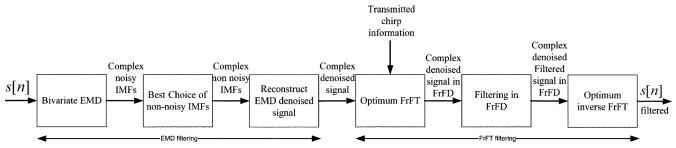

Fig. 3. EMD-FrFT filtering.

by the dot product of the chirp signal by the Doppler vector $\boldsymbol{F}_d$ defined as

$$\boldsymbol{F}_d = \exp\left(j2\pi f_d(t - T_{start})\right) \tag{12}$$

where f_d is the target Doppler frequency.

For the phased array receiving antenna, an antenna phase factor $\boldsymbol{F}_\phi$ is introduced as

$$\boldsymbol{F}_\phi = \exp\left(-j2\pi f_c(T_{start}\boldsymbol{I} - \boldsymbol{N_{array}}\Delta t)\right) \tag{13}$$

where $\boldsymbol{N_{array}}$ is a vector represented as $\{0, 1, \ldots\ldots, N-1\}$, $\boldsymbol{I}$ is a $1 \times N$ unitary vector, and Δt is calculated from

$$\Delta t = D \sin \phi_t / c \tag{14}$$

where D is the separation between the antenna elements, ϕ_t is the target angle from the antenna boresight.

V. Filtering Based EMD-FrFT Algorithm

It is proposed to combat the high power noise interference by filtering the received signal in the optimal fractional Fourier transform (FrFT) domain using the transmitted chirp radar information. Normally the magnitude of chirp signal in the optimum FrFT domain would be significantly higher than the noise signal in the fractional domain [1]. However in high power jamming scenarios this is not usually true and it becomes difficult to distinguish between the target spike and the noise spikes in the optimal FrFT domain.

The proposed EMD-FrFT radar filtering process, which must be applied to the received signal before the band pass filter, is shown in Fig. 3. The radar received noisy complex chirp signal $s(t)$ is sampled using the radar sampling frequency to form $s[n]$. The $s[n]$ signal recovery is carried out in two stages: i) EMD Filtering Stage and ii) the FrFT Filtering Stage.

EMD Filtering Stage: In stage one the received signal $s[n]$ is input to a bivariate EMD to produce the complex IMFs $\boldsymbol{h}^{(i)}[n]$. The complex IMFs are detrended and thresholded to estimate the non-noisy IMFs using (2)–(5) as described in Section II. Only IMFs whose energy exceeds the threshold are retained. The resultant thresholded IMFs are combined to produce the complex denoised signal as in (6).

FrFT Filtering Stage [1]: For the second stage, the complex denoised signal in the optimal fractional domain is calculated from the information supplied from the transmitted chirp signal as in (8). Knowing the peak position of the target chirp signal in the optimum FrFT domain, the received data is filtered by keeping the chirp target data (peak position sample and its adjacent samples) and forces all the remaining samples in the tracking window to zero. The inverse FrFT is used with the known optimal order to transform the signal back to time domain after filtering. The EMD-FrFT filtered data is supplied to the radar processor to continue data processing to calculate the target information.

The EMD-FrFT filtering process illustrated in Fig. 3 is attached to N receiving channels in which the received signal from each of the N antenna elements will fill L_s range gates.

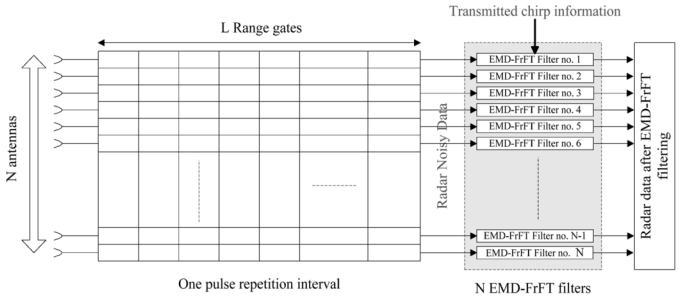

Fig. 4. Radar data EMD-FrFT filtering.

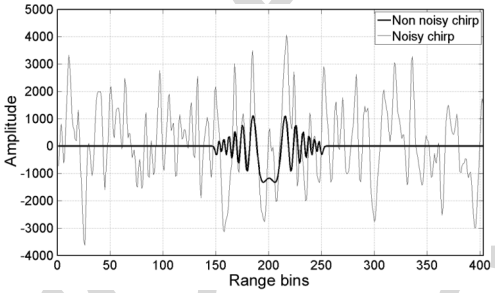

Fig. 5. High noisy chirp signal in time domain (real).

The total radar data size is therefore equal to $N \times L_s$ for each pulse return. The EMD-FrFT filter block seen in Fig. 4 consists of N EMD-FrFT filters shown in Fig. 3. The overall filtered data $(N \times L_s)$ are processed to determine the target information parameters as illustrated in Fig. 2.

VI. Simulation Results

The computer based simulations comprise an array of 14 elements spaced 1/3 m apart. The radar pulse width is 100 microseconds and a pulse repetition interval of 1.6 ms for a 435 MHz carrier was used. The incoming baseband signals are sampled at 1 MHz. Also it is assumed that the radar operating range is 100:200 range bins with a starting window at 865 μm and a window duration of 403 μm. The target is considered at range bin $=$ 150 at angle 32° from the look direction with target signal to noise ratio (SNR) set to 56 dB. A jamming signal with interference noise ratio (INR) set to 75 dB at angle 32° from the look direction (main beam jamming) is introduced.[1]

A. High Power Interference Scenario

Considering the simulation parameters for one of the 14 receiving channels (first channel), the receiving target chirp signal appears at range bin 150 in case of no jamming while the chirp signal is completely corrupted in the time domain (also in the frequency domain) by the noise due to high power jamming signal as seen in Fig. 5.

The bivariate EMD is applied to the noisy signal to produce the complex IMFs. A sampling frequency is increased to 10 MHz (ten times the radar sampling frequency F_s) to increase the number of IMFs.

The resultant complex IMFs from applying the bivariate EMD to the noisy chirp 1×4029 produces 14 IMFs each of length 4029. Keeping only IMFs whose energy exceeds the threshold using the EMD-DT algorithm described in Section II the signal is reconstructed summing the non-noisy IMFs from

[1]The simulations parameters are extracted from DARPA/Navy Mountaintop Program. See URL http://spib.rice.edu/spib/mtn_top.html.

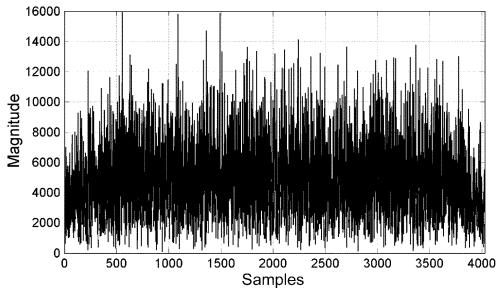

Fig. 6. High noisy chirp signal in optimum FrFD.

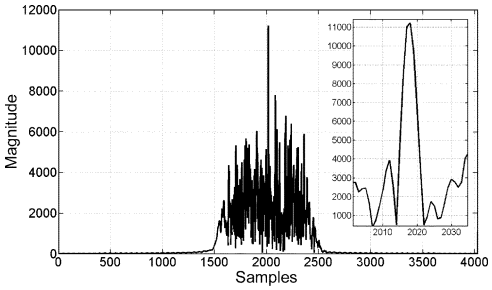

Fig. 7. EMD denoised chirp in optimum FrFD.

6 to 14 to obtain the filtered signal after applying EMD-DT algorithm.

Substituting the monopulse radar parameter values given above into (8) with a high sampling frequency of 10 MHz, the order of the optimal FrFT domain a_{opt} is computed as 1.1266. The EMD filtered signal is transferred to the optimal FrFD using the optimal order FrFT domain a_{opt} 1.1266.

Transforming the radar received signal directly to the optimum FrFD using the calculated a_{opt}, is expected to produce a high magnitude value (spike) due to transferring the chirp signal to the optimum FrFD. However as seen in Fig. 6 due to the high power interference the spike of the target chirp is highly corrupted also by noise spikes in the optimum FrFD and cannot be filtered in this domain.

It is therefore difficult to distinguish between the target spike and the noise spikes in the optimal FrFD. The proposed EMD-FrFT filtering algorithm is used to address this problem. Fig. 7 shows the EMD denoised chirp in optimum FrFD. It is evident that the noise is significantly reduced especially the high frequency components and the chirp target spike is also the highest spike which is shown in the zoomed portion of Fig. 7.

The proposed filtering algorithm in the optimum FrFD keeps the sample with maximum magnitude (sample no. 2018) and its ten adjacent samples from 2013–2023 while forcing all other samples window to zero. The filtered signal is then transformed back to time domain by applying inverse optimum FrFT using—a_{opt} (-1.1266) by applying (7). The real and imaginary parts of the denoised signal (recovered) after applying the proposed EMD-FrFT filtering algorithm is shown in Fig. 3.

Fig. 8 compares the denoised chirp signal using EMD-FrFT filter with the non noisy signal. In the simulation example, the considered signal total input SNR is approximately equal -8 dB (after adding the jamming noise) and the output SNR is approximately 10 dB. The proposed EMD-FrFT filtering algorithm offers signal enhancement of approximately 18 dB.

B. Signal Improvement at Different SNR

Table I shows the improvement results of applying different target SNR for the same jamming scenario (INR set to 75 dB

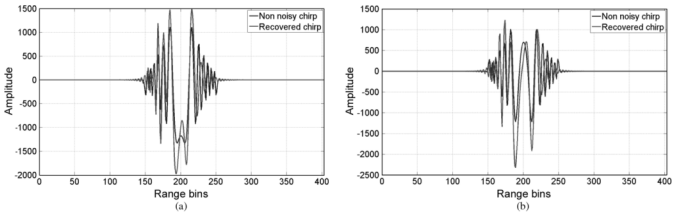

Fig. 8. Recovered chirp signal. (a) Real; (b) imaginary.

TABLE I
THE IMPROVEMENT RESULTS IN dB FOR MONOPULSE PROCESSORS

Input SNR	**-7.7**	**-5.6**	**-2.9**	**-1.8**	**0.2**	**1.7**	**5.6**	**10.6**
Output SNR	**10.4**	**10.8**	**13**	**13.4**	**14.8**	**15.4**	**15.8**	**15.5**
Gain	**18.1**	**16.4**	**15.9**	**15.2**	**14.6**	**13.7**	**10.2**	**4.9**

at angle 32°) and calculating the total input SNRs to the radar receiving channel. The results in Table I comprise an average over 50 independent noise generations.

Table I indicates an improvement of approximately 18.1 dBs for input SNR $= -7.7$ dB and an improvement of approximately 4.9 dBs for input SNR $= 10.6$ dB. The proposed EMD-FrFT algorithm yields a higher improvement for the lower SNRs rather than the higher SNRs.

VII. CONCLUSION

A system to reduce the distortion problem due to high power interference in chirp radar systems is presented. The proposed EMD-FrFT filtering algorithm successfully decreases the high power noise interference and improves the received radar SNR. A resulting improvement in the radar received signal is obtained for different SNR and the highest gain is achieved in the case of lower SNR (up to 18 dB in the considered case).

REFERENCES

[1] S. A. Elgamel and J. J. Soraghan, "Enhanced monopulse radar tracking using fractional fourier filtering in the presence of interference," in *11th Int. Radar Symp. (IRS), 2010 11th International*, 2010, pp. 1–4.

[2] A. Farina, G. Golino, and L. Timmoneri, "Maximum likelihood estimator approach to determine the target angular co-ordinates in presence of main beam interference: Application to live data acquired with a microwave phased array radar," in *IEEE Int. Radar Conf.*, 2005, pp. 61–66.

[3] Y. Seliktar, E. J. Holder, and D. B. Williams, *A Space/Fast-Time Adaptive Monopulse Technique*. New York: Hindawi, 2006, pp. 218–228.

[4] J. Zongsheng and S. Xicai, "Analysis on the tracking performance of active radar seeker under the condition of coherent interference," in *IEEE Int. Conf. Intelligent Computing and Intelligent Systems*, 2009, pp. 418–422.

[5] P. Flandrin, P. Goncalves, and G. Rilling, "Detrending and denoising with empirical mode decompositions," in *2004 Eur. Signal Processing Conf. (EUSIPCO-2004)*, 2004.

[6] G. Rilling, P. Flandrin, P. Gonalves, and J. M. Lilly, "Bivariate empirical mode decomposition," *IEEE Signal Process. Lett.*, vol. 14, pp. 936–939, 2007.

[7] C. Candan, M. A. Kutay, and H. M. Ozaktas, "The discrete fractional fourier transform," *IEEE Trans. Signal Process.*, vol. 48, pp. 1329–1337, 2000.

[8] H. M. Ozaktas, G. Zalevsky, and M. A. Kutay, *The Fractional Fourier Transform: With Applications in Optics and Signal Processing*. New York: Wiley, Jan. 2001.

[9] C. Capus and K. Brown, "Short-time fractional fourier methods for the time-frequency representation of chirp signals," *J. Acoust. Soc. Amer.*, vol. 113, no. 6, pp. 3253–3263, 2003.